Hindawi
Journal of Combustion
Volume 2021, Article ID 6642734, 15 pages
https://doi.org/10.1155/2021/6642734

Research Article

A Detailed Numerical Study of NOx Kinetics in Counterflow Methane Diffusion Flames: Effects of Fuel-Side versus Oxidizer-Side Dilution

Huanhuan Xu,[1] **Fengshan Liu**,[2] **Zhiqiang Wang**,[1] **Xiaohan Ren**,[3] **Juan Chen**,[1] **Qiang Li**,[4] **and Zilin Zhu**[1]

[1]*National Engineering Laboratory for Reducing Emissions from Coal Combustion, School of Energy and Power Engineering, Shandong University, Jinan 250061, China*
[2]*Measurement Science and Standards, National Research Council Canada, Building M-9 1200, Montreal Road, Ottawa, ON K1A 0R6, Canada*
[3]*Institute of Thermal Science and Technology, Shandong University, 17923 Jingshi Road, Jinan 250061, Shandong, China*
[4]*College of Chemical Engineering, China University of Petroleum (East China), Qingdao 266580, China*

Correspondence should be addressed to Zilin Zhu; zilinzhu323@gmail.com

Received 14 October 2020; Revised 19 February 2021; Accepted 21 February 2021; Published 3 March 2021

Academic Editor: Siamak Hoseinzadeh

Dilution combustion has been widely utilized due to various merits, such as enhanced efficiency, fewer pollutants emissions, and even a promising future in alleviating global warming. Diluents can be introduced through the oxidizer or fuel side to achieve the desired combustion properties, and H_2O and CO_2 are the most common ones. A comprehensive comparison between the different dilution methods still lacks understanding and optimizes the dilution combustion technologies. This study numerically compared the effects of H_2O and CO_2 dilution in the oxidizer or fuel stream on counterflow methane diffusion flames, emphasizing NO formation kinetics. Results showed that the impact of different radiation heat transfer models on NO emissions diminishes with increasing the dilution ratio. The calculations of radiation heat transfer were treated in three ways: radiation-neglected, optically thin, and using a nongrey radiation model. When keeping the oxygen content and methane fraction constant, CO_2 dilution in the air-side has the most profound influence on NO reduction, and CO_2 dilution in the fuel-side has the least. H_2O dilution showed a medium impact with a larger degree on air-side than that on fuel-side. To gain a deeper understanding of this effect order, the contributions of different NO formation routes were quantified, and analyses were made based on the diluents' chemical and thermal effects. It was found that the oxidizer-side dilution and fuel-side dilution affect the NO formation pathway similarly. Still, the influence of H_2O dilution on the NO formation pathway differs from that of CO_2 dilution.

1. Introduction

Several advanced combustion technologies have been proposed to address the challenges of both fossil fuel depletion and environmental pollution. Additives are widely used to enhance combustion efficiency, control nitric oxide emissions, or achieve low-cost CO_2 capture. For example, humidified air turbines (HATs) [1] with a mixture of air and water as the working fluid promise high electrical efficiencies and low NOx emissions. Fossil fuels combust with pure oxygen in a Graz Cycle Gas Turbine [2] by using CO_2 to control the flame temperature, enabling the cost-effective separation of the CO_2 in flue gas physical condensation. In combustion technologies based on exhaust gas recirculation (EGR) [3], part of the exhaust gas (mainly H_2O and CO_2) is introduced back to the combustion chamber, and NOx emissions could be substantially reduced. Internal Combustion Rankine Cycle (ICRC) power plants [4] run under an oxy-fuel combustion model with recycled water to achieve high efficiency and specific power output. Other systems using water to provide power can be found in [5, 6].

To gain the full potential benefits of dilution combustion, it is crucial to understand the effects of the following three primary factors: (1) the type of diluents, (2) the amount of dilution, and (3) the location (oxidizer or fuel stream) where the diluents are injected.

Among the various combustion technologies mentioned above, carbon dioxide and steam (water vapor) are the most common additives. As H_2O and CO_2 are two main combustion products, adding these two diluents to the combustion zone will not introduce new species but increase H_2O and CO_2 concentrations in the flue gas. As a result, CO_2 capture becomes much more manageable and economical. Besides, the high heat capacity of H_2O and CO_2 enables many favorable combustion properties, such as low flame temperature [7, 8] and low NOx emissions [9]. To grasp the dilution mechanism of H_2O and CO_2, many efforts have been made. For example, Park et al. [10] simulated the flame structure and NO emission behavior in CH_4 diffusion flames with different diluents (H_2O, CO_2, and N_2) added to the air stream. Their results showed that CO_2 addition reduces the flame temperature through both the thermal and chemical effects. In contrast, the addition of H_2O enhances the reaction through chemical effect and limits the decrease of temperature thermally. They also pointed out that the NO emission index decreases with increasing the volume percentage of diluents. The effectiveness of these diluents on NO emission reduction follows the order of $CO_2 > H_2O > N_2$. Xie et al. [11] found that the elementary reaction corresponding to the peak ROP (rate of production) of OH in CO/H_2/air mixture changes from $OH + H_2 = H + H_2O$ to $HO_2 + H = OH + OH$ when CO_2 and H_2O are added, and CO_2 has a more potent chemical effect than H_2O. Xu et al. [8] investigated the effects of H_2O and CO_2 diluted oxidizer on the structure and shape of laminar co-flow syngas diffusion flames. They found that the thermal and radiative effects of CO_2 decrease the centerline temperature to a much larger degree than those of H_2O; thus, CO_2 reduces the centerline temperature more effectively than H_2O. Besides, they also found that as the dilution level increases, the maximum OH mole fraction in CO_2 diluted flames decreases monotonously, whereas in H_2O diluted flames, OH mole fraction first increases then decreases. Ning et al. [12] numerically studied the radiation effect on NO formation in H_2/CO/air counterflow diffusion flames, and results showed that, as the CO_2 content in the fuel stream increases, the radiation effect on NO emission increases first and then decreases for H_2-lean syngas. In contrast, for H_2-rich syngas, the radiation effect is monotonic. Ozturk [13] studied the effects of CO_2, N_2, and H_2O dilution on the adiabatic, turbulent, partially premixed combustion of synthesis gas and pointed out that increasing the dilution rates gradationally reduces the NO concentration and H_2O has the best effect on reduction of NO emissions, followed by CO_2 and N_2. Although these studies help fundamental understanding of the influence of diluents and dilution level on the combustion characteristics of hydrocarbon fuels, they were conducted for either fuel-side dilution or air-side dilution. They hence did not provide a direct comparison of the relative effectiveness between fuel-side dilution and oxidizer-side dilution.

Researchers have made a few attempts to explore the difference between air- and fuel-side dilutions for jet diffusion flames. For instance, Feese and Turns [14] experimentally studied the effects of N_2 dilution in the air- or fuel-side on NOx emissions in laminar CH_4 jet diffusion flames. They found that air dilution was more effective than fuel dilution in reducing NOx emissions. They also pointed out that the visible flame height increases somewhat as a diluent is added to the airstream but does not change noticeably for fuel-side dilution, even for the same diluent fraction. Unfortunately, Feese et al. did not analyze the NO formation routes or provide kinetic explanations for their results. In addition, an experimental study by Cho and Chung [15] showed that fuel-side dilution is more effective in reducing flame temperature and NO emissions than air-side dilution. It should be noted that, although Cho and Chung also studied jet diffusion flames, they reached a different conclusion from that in [14]. This contradiction is due to the different dilution parameters used in these two studies when comparing the fuel-side dilution and the air-side dilution. In Cho and Chung's study [15], the dilution ratio was defined as the ratio of the exhaust gas flow rate to the total flow rate of the fuel (or air). Because the fuel stream's exit area is much smaller than that of the oxidizer stream, the fuel stream velocity increases more than the oxidizer stream velocity increases. The much higher increase in fuel stream velocity enhances the mixing in dilution combustion. In the study of Feese and Turns, however, they introduced a new dilution parameter (Z), calculated as the mass of diluent to the stoichiometric mixture's mass. In this way, under the same Z, the amount of diluent added to the air stream for air-side dilution is much more considerable than that added to the fuel stream for fuel-side dilution.

The effect of dilution on NO formation is one of the issues this study aimed to resolve since one of the advantages of dilution combustion is the low NO emissions, which is strongly dependent on the combustion conditions, reported in the previous papers, i.e., Refs. [16–18].

To obtain a fundamental understanding of the effect of dilution position (i.e., through air or fuel stream) on flame characteristics, attention has also been paid to one-dimensional diffusion flames, which excludes the burner's complexity and flow field in multidimension flames. Using spherical diffusion flames, Chernovsky et al. [19] experimentally investigated the impact of adding CO_2 on the oxidizer side versus the fuel side. Their results showed that CO_2 dilution affects the flame in these two dilution scenarios by different mechanisms. On the oxidizer side, radiation reabsorption played an essential role in strengthening the flames. In contrast, the enhanced CO_2 concentration increased radiative heat losses on the fuel-side without prompting radiation reabsorption. Park et al. [20] numerically investigated the effects of CO_2 addition to the fuel and the oxidizer streams on the structure of H_2/O_2 diffusion flame in counterflow configuration, and results showed that the temperature reduction caused by the chemical effects is more remarkable when CO_2 is added to the oxidizer stream than that to the fuel stream. Liu et al. [21] numerically studied the chemical effects of CO_2 addition to both the fuel side and the oxidizer side of a laminar counterflow ethylene

diffusion flame. The study of Liu et al. is highly relevant to the present study, and their results showed that the chemical effects of CO_2 are weaker when added to the fuel side than to the oxidizer side. NOx formation pathway analyses are essential to reveal how CO_2 addition affects NOx formation mechanisms; however, Liu et al. did not conduct this work but only focused on the chemical effects of CO_2.

Despite several studies that have been conducted to understand the difference between fuel- and air-side dilutions, there is still a lack of comprehensive comparison between H_2O dilution and CO_2 dilution in the fuel- and oxidizer side. Many questions remain unanswered regarding NO emissions, such as the radiation effect on NO emissions and the chemical effect of diluents on the NO formation mechanism. To this end, the objectives of this study were to investigate the influence of H_2O and CO_2 dilution in the air and fuel stream on methane/air counterflow diffusion flames with an emphasis on the detailed NO formation process, including not only the formation and destruction routes, but also the reaction pathway analysis. The importance of gas radiation in modeling the methane/air diffusion flames was first demonstrated for different diluting levels and in the air and fuel stream with H_2O or CO_2. The effects of H_2O and CO_2 dilutions in the fuel and air stream on flame temperature and NO concentration were next examined by adopting the DOM/SNBCK radiation model. The diluents' chemical effects and thermal effects were isolated and analyzed. Finally, to reveal the impact of different diluents and dilution locations (air or fuel stream) on the NO formation mechanism, the contributions of different NO formation routes were calculated, and the NO formation pathways were revealed.

2. Mathematical Model and Numerical Methods

2.1. Simulation Methods. The OPPDIF code [22] coupled with the thermal and transport subroutines in the CHEMKIN package [23] was adopted in this study to compute the counterflow diffusion flames. This code has been extensively validated and used to model one-dimensional laminar flames (nonpremixed or premixed) using detailed combustion chemistry and thermal and transport properties. The methane oxidation chemistry was modeled using the GRI-Mech 2.11 mechanism [24]. Many studies [25, 26] have demonstrated that GRI-Mech 2.11 produces a better prediction for NOx formation than the GRI-Mech 3.0 mechanism when modeling methane combustion. To illustrate the importance of radiation heat transfer, three different treatments of thermal radiation were considered, namely, no radiation heat loss, the optically thin approximation (OTA) [27], and the discrete-ordinates method (DOM) coupled with the statistical narrow-band correlated-K-based radiative property model (DOM/SNBCK) for solving the radiative transfer equation (RTE) [28]. The OTA only accounts for radiation loss due to emissions. It neglects radiation gain by absorption, while the DOM/SNBCK model considers both radiation emission and absorption, as well as the non-gray nature of gas radiative properties. Multicomponent transport properties and thermal diffusion were considered to deal with the preferential diffusion of H_2 and H. The grid adaptation parameters of GRAD and CURV were both set to 0.05 to ensure that the computational meshes are sufficiently refined, and the simulation results are grid size independent. The global strain rate a_s defined in equation (1) is fixed at $50\,s^{-1}$ for the flames modeled in this paper unless otherwise indicated. The fuel and oxidizer streams' outlet velocities were chosen to satisfy the momentum balance [29] expressed in equation (2):

$$a_s = \frac{2|V_O|}{L}\left(1 + \frac{|V_F|\sqrt{\rho_F}}{|V_O|\sqrt{\rho_O}}\right), \tag{1}$$

$$\rho_O V_O{}^2 = \rho_F V_F^2, \tag{2}$$

where ρ and V represent the density and velocity, respectively, and the subscripts "F" and "O" indicate the fuel and oxidizer streams. Symbol L is the distance between the fuel and oxidizer nozzles, specified as 2 cm in this study.

2.2. Simulation Conditions. The flame conditions investigated in this study are summarized in Table 1. It is worth pointing out that when a certain amount of diluent (H_2O or CO_2) was added to the fuel or the oxidizer stream, the same amount of N_2 was removed; therefore, the CH_4 and O_2 mole fractions could keep unchanged at 50 vol% and 21 vol% in the fuel and oxidizer stream, respectively. The pressure was 1 atm, and the inlet temperature of both the oxidizer and fuel streams was ranged from 400 K to 800 K in this study.

2.3. NO Formation Mechanism. To identify the contributions of different NO formation routes, NO is considered to be formed by four pathways and destructed through NO-reburning. First, the thermal NO is formed through the N_2 triple bond break-up by the O atom, and O_2 and OH subsequently oxidize the N atom. This process has very high activation energy and is strongly affected by flame temperature. The main reactions related to NO formation in the GRI-Mech 2.11 mechanism are listed in Table 2. Reactions responsible for thermal NO include R178, R179, and R180. Second, the prompt NO can be prevalent in hydrocarbon flames since it is produced via reactions of CH*i* radicals, and R240 is usually considered as the major initiation step for the formation of prompt NO. The reactions involved in prompt NO are rate-limiting, leading to the prompt NO formation less temperature-dependent. Third, the N_2O-intermediate NO is formed through the path of $N_2 \longrightarrow N_2O \longrightarrow NO$, with N_2O being the intermediate species. Fourth, the NNH NO begins with N_2 reacting with H to form NNH (R204 and R205), which then yields NO through R208. Lastly, NO-reburning is an important destruction mechanism of NO by a group of reactions involving hydrocarbon radicals, CH_i. The calculation method of these NO formation routes has been widely employed in previous studies, e.g., Refs. [27, 30, 31].

The full GRI-Mech 2.11 mechanism contains 49 species and 279 elementary reactions, and the number of reaction steps decreases to 177 when excluding NO formation. For

Table 1: Conditions of diluted methane/air counterflow diffusion flames with and without H_2O or CO_2 replacement of N_2, 400 K, 1 atm.

No.	Fuel stream composition (vol%)				Oxidizer stream composition (vol%)				Remark
	CH_4	N_2	H_2O	CO_2	O_2	N_2	H_2O	CO_2	
Case 1	50	50	0	0	21	79	0	0	Baseline H_2O dilution (fuel-side)
Case 2	50	40	10	0	21	79	0	0	
Case 3	50	30	20	0	21	79	0	0	
Case 4	50	10	40	0c	21	79	0	0	
Case 5	50	40	0	10	21	79	0	0	CO_2 dilution (fuel-side)
Case 6	50	30	0	20	21	79	0	0	
Case 7	50	10	0	40	21	79	0	0	
Case 8	50	50	0	0	21	69	10	0	H_2O dilution (air-side)
Case 9	50	50	0	0	21	59	20	0	
Case 10	50	50	0	0	21	39	40	0	
Case 11	50	50	0	0	21	69	0	10	CO_2 dilution (air-side)
Case 12	50	50	0	0	21	59	0	20	
Case 13	50	50	0	0	21	39	0	40	

Table 2: Main reactions involved in NO formation (more information can be found in the GRI-Mech 2.11 mechanism [24]).

Reaction no.	Reaction steps	Reaction no.	Reaction steps
R178	$N + NO => N_2 + O$	R179	$N + O_2 \leq NO + O$
R180	$N + OH = NO + H$	R182	$N_2O + O \leq 2NO$
R183	$N_2O + H = N_2 + OH$	R185	$N_2O(+M) \leq N_2 + O(+M)$
R186	$HO_2 + NO = NO_2 + OH$	R187	$NO + O + M = NO_2 + M$
R189	$NO_2 + H = NO + OH$	R190	$NH + O = NO + H$
R191	$NH + H = N + H_2$	R192	$NH + OH = HNO + H$
R193	$NH + OH = N + H_2O$	R194	$NH + O_2 = HNO + O$
R195	$NH + O_2 = NO + OH$	R197	$NH + H_2O = HNO + H_2$
R199	$NH + NO = N_2O + H$	R201	$NH_2 + O = H + HNO$
R202	$NH_2 + H = NH + H_2$	R203	$NH_2 + OH = NH + H_2O$
R204	$NNH = N_2 + H$	R205	$NNH + M = N_2 + H + M$
R206	$NNH + O_2 = HO_2 + N_2$	R207	$NNH + O = OH + N_2$
R208	$NNH + O = NH + NO$	R209	$NNH + H = H_2 + N_2$
R210	$NNH + OH = H_2O + N_2$	R212	$H + NO + M = HNO + M$
R213	$HNO + O = NO + OH$	R214	$HNO + H = H_2 + NO$
R215	$HNO + OH = NO + H_2O$	R216	$HNO + O_2 = HO_2 + NO$
R217	$CN + O = CO + N$	R218	$CN + OH = NCO + H$
R219	$CN + H_2O = HCN + OH$	R220	$CN + O_2 = NCO + O$
R221	$CN + H_2 = HCN + H$	R223	$NCO + H = NH + CO$
R231	$HCN + O = NCO + H$	R232	$HCN + O = NH + CO$
R234	$HCN + OH = HOCN + H$	R235	$HCN + OH = HNCO + H$
R236	$HCN + OH = NH_2 + CO$	R240	$CH + N_2 = HCN + N$
R246	$CH + NO = HCN + O$	R249	$CH_2 + NO = H + HNCO$
R250	$CH_2 + NO = OH + HCN$	R251	$CH_2 + NO = H + HCNO$
R255	$CH_3 + NO = HCN + H_2O$	R265	$HNCO + H = NH_2 + CO$
R270	$HCNO + H = H + HNCO$	R272	$HCNO + H = NH_2 + CO$
R273	$HOCN + H = H + HNCO$	R274	$HCCO + NO = HCNO + CO$

clarity, we abbreviate these two mechanisms as "he full GRI-Mech 2.11 mechanism conta respectively. To quantify NO formation from the four formation routes plus one destruction route, each simulation was performed six times with different NO formation kinetics models, namely, "Full chemistry" (marked as SIM1), "no NO chemistry" with only the thermal, prompt, NNH, or N_2O-intermediate NO formation route, marked as SIM2 ~ SIM5, respectively, and "Full chemistry" excluding NO-reburning route (SIM6). The elementary steps involved in calculating each NO formation route are identical to these in Ref. [30]. As a result, NO formations through the thermal, prompt, NNH, or N_2O-intermediate routes can be obtained by subtracting results of the corresponding SIM2~SIM5 with that of the SIM1. NO-reburning effect on NO was calculated by the difference in results of SIM6 and SIM1.

2.4. Chemical and Thermal Effects of H_2O/CO_2. To quantitatively investigate the chemical and thermal effects of H_2O or CO_2 dilution, calculations with real H_2O and CO_2 and their chemically inert counterpart were conducted as we did in the previous work [8]. Specifically, this chemical effect refers to the diluents' impact through their participation the

chemical reactions. The thermal effect means the influence caused by the difference of the diluents' thermal properties from those of N_2. The two artificial species, FH_2O and FCO_2, have the same thermal, transport, and radiative properties as these of the real H_2O and CO_2, respectively, except that FH_2O and FCO_2 are chemically inert and do not participate in chemical reactions. To be specific, when evaluating CO_2 and H_2O's chemical effects, two sets of simulations were conducted. One was using the real CO_2 and H_2O as the diluent, and the other was using FCO_2 and FH_2O. Therefore, differences between results based on FH_2O and FCO_2 and those using H_2O and CO_2 are attributed to H_2O and CO_2's chemical effects. Similarly, to quantify H_2O and CO_2's thermal effects, another pair of artificial species, TH_2O and TCO_2, having the same chemical, transport, and radiative properties as FH_2O and FCO_2 but share the same thermal properties with N_2 were introduced to the reaction mechanisms. As a result, differences in the numerical results using TH_2O (or TCO_2) additions and these using FH_2O (or FCO_2) additions are caused by H_2O and CO_2's thermal effects.

3. Results and Discussion

3.1. Effect of Radiation Models. Since H_2O and CO_2 are the most critical radiative gases in hydrocarbon combustion, it is expected that H_2O and CO_2 enhance radiation heat transfer in the combustion zone. The results calculated using the three radiation models were first examined to investigate radiation treatment's effect on modeling the different diluted flames. Figure 1 displays the predicted peak flame temperatures using the three radiation heat transfer treatments for CO_2 and H_2O dilution added to the fuel and air streams. Some common behaviors can be observed from this figure. For example, CO_2 dilution has a more decisive influence than H_2O dilution due to its higher specific heat capacity per volume [7, 8]. As expected, neglecting the thermal radiation results in overprediction of flame temperature, while OTA under predicts the peak flame temperature. Since the DOM/SNBCK model considers both emission and absorption of radiation, it predicts the peak flame temperature lower than that of no radiation but higher than OTA. It is interesting to notice that the peak temperature predicted by DOM/SNBCK is much closer to that of no radiation, suggesting that there is significant radiation reabsorption in flames to reduce the net radiation loss. These results also show that the air-side dilution (black lines) has a stronger influence on suppressing the flame temperature than the fuel-side dilution (red lines). Kinetics analysis shows this is attributed to that the heat release rate of reactions $O + C_2H_2 = CO + CH_2$ and $H + O_2 + H_2O = HO_2 + H_2O$ is more suppressed when dilution occurs at the air-side than that at the fuel-side. In particular, an interesting phenomenon observed in Figure 1 is that the impact of H_2O and CO_2 dilution on the peak flame temperature is nearly linear for dilution ratio up to 40%, no matter dilution occurs in the fuel side or the air-side.

The effects of radiation models on the predicted peak NO mole fractions for CO_2 and H_2O dilution on the fuel and air stream are shown in Figure 2. The variation of peak NO mole fraction with dilution ratio is clearly nonlinear.

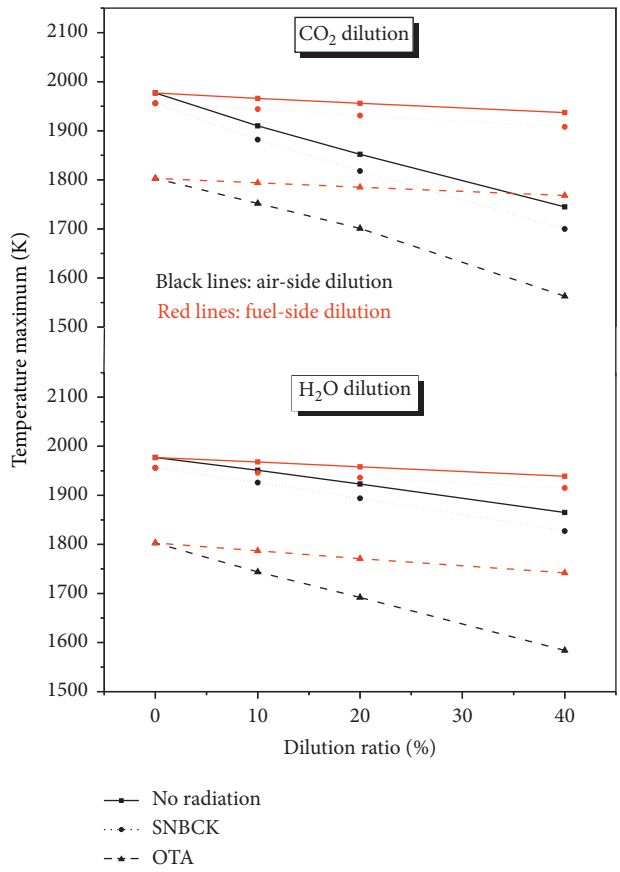

Figure 1: Variation of the peak flame temperature of CH_4/air counterflow diffusion flames with the dilution ratio for H_2O and CO_2 addition to the air and fuel side: $a_s = 50\ s^{-1}$, $L = 2$ cm, 400 K.

Besides, the radiation model's effect on the NO mole fraction is quite significant. Consistent with the radiation model's effects on the peak flame temperature, when neglecting the radiation heat transfer, OTA predicts the lowest NO mole fraction. At a given flame condition, the NO mole fraction predicted by the DOM/SNBCK model falls between no radiation and OTA but closer to no radiation. However, the radiation model's effect on the predicted peak NO mole fraction weakens with increase in the dilution ratio, especially for the air-side dilution. As shown in Figure 2, when dilution occurs in the air-side (black lines), both H_2O dilution and CO_2 dilution reduce the peak NO mole fraction significantly; however, the reduction rate continuously weakens as the dilution ratio increases. The different influence of dilution on the peak NO mole fraction form the impact on the peak flame temperature, i.e., the nonlinear reduction of the peak NO mole fraction in Figure 2 and nearly linear reduction in the peak flame temperature in Figure 1, implies that the temperature-sensitive thermal NO route is not the primary pathway for NO formation under the conditions of this study. This point will be discussed later. Since the effect of fuel-side dilution on the NO mole fraction maximum is much weaker than that of air-side dilution, the nonlinear trend is not pronounced, especially for CO_2 dilution on the

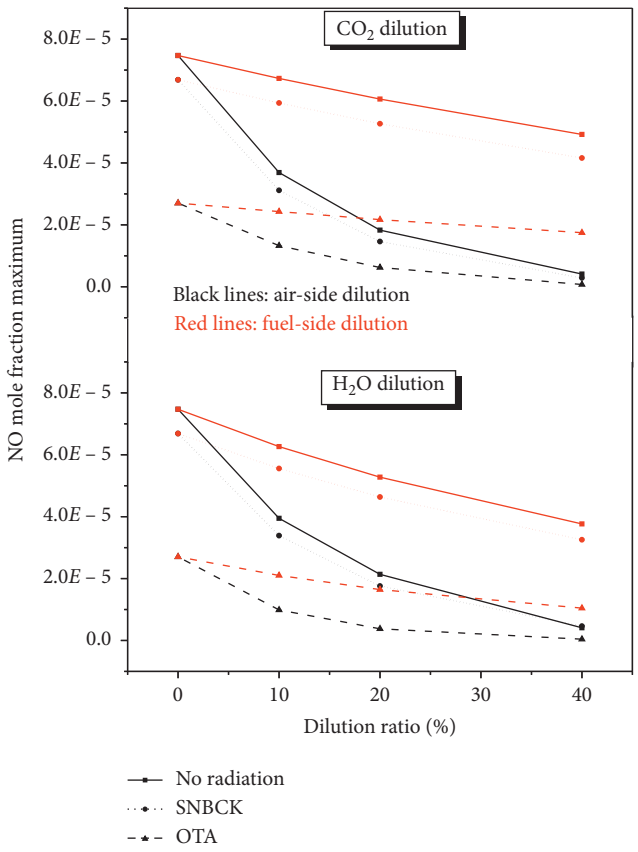

FIGURE 2: Variation of the peak NO mole fraction of CH_4/air counterflow diffusion flames with the dilution ratio by H_2O and CO_2 dilution on the air and fuel side: $a_s = 50\ s^{-1}$, $L = 2$ cm, 400 K.

fuel-side. For the fuel-side dilution, thermal NO is not the dominant route, as illustrated in Section 3.4.

3.2. Flame Temperature. From this section, the numerical results were calculated using the DOM/SNBCK radiation model since this radiation treatment provides the most accurate treatment of radiation heat transfer. In this part, the influence of H_2O and CO_2 dilution on flame temperature is discussed in detail. Figure 3 displays the temperature distributions for H_2O and CO_2 dilution up to 40% on the fuel and air-side as a function of the distance from the fuel nozzle. The differences in the peak flame temperature between Case 1 (no dilution) and the cases of 40% H_2O and 40% CO_2 dilution are also indicated. Although H_2O and CO_2 dilution on either the air or the fuel-side lowers the flame temperature consistently, differences between H_2O dilution and CO_2 dilution still exist. First, CO_2 is more effective than H_2O in reducing the flame temperature, regardless of if it being added to the air or the fuel side. This difference is mainly caused by the higher heat capacity of CO_2. Second, H_2O dilution always slightly shifts the peak flame temperature towards the air nozzle, but CO_2 dilution can shift the peak temperature slightly towards either the fuel nozzle or the oxidizer nozzle when, respectively, added to the fuel or air stream. This difference is related to the relative molar weights of N_2, H_2O, and CO_2. Nevertheless, the flame sheet almost remains at the same position since the momentum was balanced by equation (2) in all the cases.

To gain further insights into how H_2O and CO_2 dilution affect the flame temperature, Figure 4 shows the separate effects of 20% H_2O and 20% CO_2 dilution to the air and fuel side on the peak temperature. The chemical and thermal effects were analyzed in this paper since the transport and radiation effects are less important [8], though the radiation effect can become significant at low strain rates. It can be seen that the thermal effects of both H_2O and CO_2 dilution reduce the flame temperature. Although the chemical effect of CO_2 lowers the flame temperature, the chemical effect of H_2O increases it, albeit only slightly. This finding agrees with that reported in the previous studies [7, 8]. Besides, Figure 4 also shows that the dilution position (air-side or the fuel-side) does not change the individual effects of H_2O and CO_2 dilution on flame temperature qualitatively, namely, the chemical effects of CO_2 and the thermal effects of H_2O and CO_2 always lower the flame temperature while the chemical effect of H_2O slightly increases it. In addition, both the overall and individual effects of H_2O and CO_2 dilutions to the air-side are greater than those to the fuel-side. Kinetics analyses show that it is because that heat released by reactions $O + C_2H_2 = CO + CH_2$ and $H + O_2 + H_2O = HO_2 + H_2O$ is more suppressed when dilution occurs at the air-side than that at the fuel-side.

3.3. NO Mole Fraction. Figures 5(a) and 5(b) present the distributions of NO mole fraction as a function of the distance from the fuel nozzle for H_2O and CO_2 dilution, respectively. It is evident that both H_2O and CO_2 dilution reduces NO formation significantly and dilution to the air stream has a stronger influence on NO reduction than the fuel side, regardless of CO_2 or H_2O dilution. The effects of CO_2 and H_2O dilution on NO mole fraction correlate well with those on flame temperature. When the air-side is diluted (red lines), CO_2 dilution suppresses NO formation more significantly than H_2O dilution, again consistent with their effects on the peak flame temperature. While for the fuel-side dilution (blue lines), the effect of H_2O dilution on suppressing NO formation is more significant than that of CO_2 dilution, which deserves further investigations because the importance of these two kinds of diluents on decreasing NO formation is opposite to that on lowering the flame temperature (Figure 3).

To understand the phenomenon that the effect of fuel-side dilution by H_2O on NO reduction is greater than that by CO_2 dilution, CH radical distributions with or without 40% H_2O and CO_2 dilution in the air- and fuel-side are compared in Figure 6. H_2O dilution on the fuel-side inhibits CH production more significantly than CO_2, which explains the greater suppression impact of H_2O dilution than CO_2 dilution on NO formation in Figure 5. Although the temperature of fuel-side CO_2 dilution is higher than that of fuel-side H_2O dilution, the significantly reduced CH concentration of fuel-side H_2O dilution slows down the initial reaction of prompt NO, i.e., $CH + N_2 = HCN + N$ (R240). Consequently, the total NO emission is inhibited

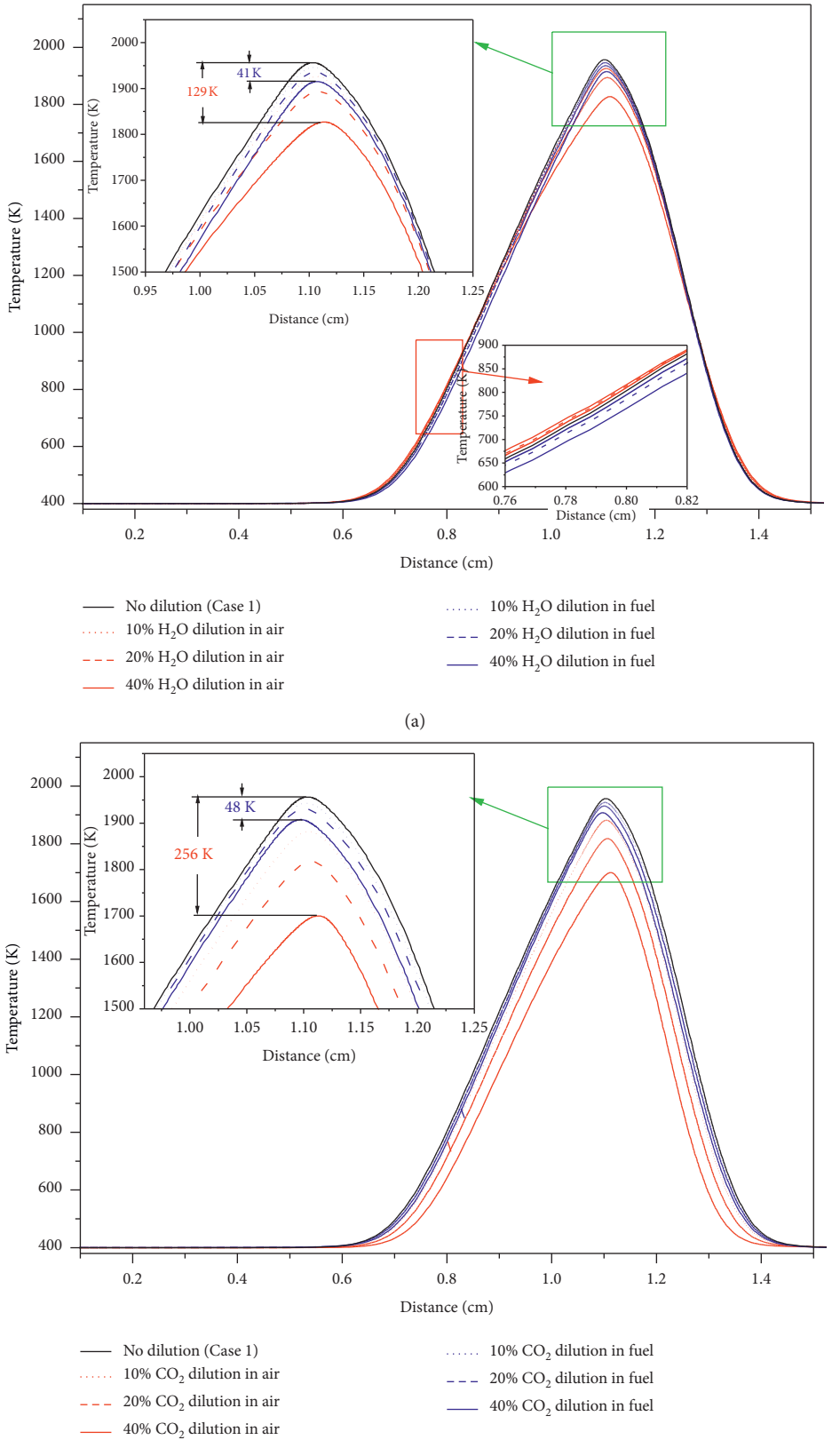

FIGURE 3: Distributions of flame temperature in CH_4/air counterflow diffusion flames with (a) H_2O dilution and (b) CO_2 dilution as a function of distance from the fuel nozzle: $a_s = 50\ s^{-1}$, $L = 2$ cm, 400 K.

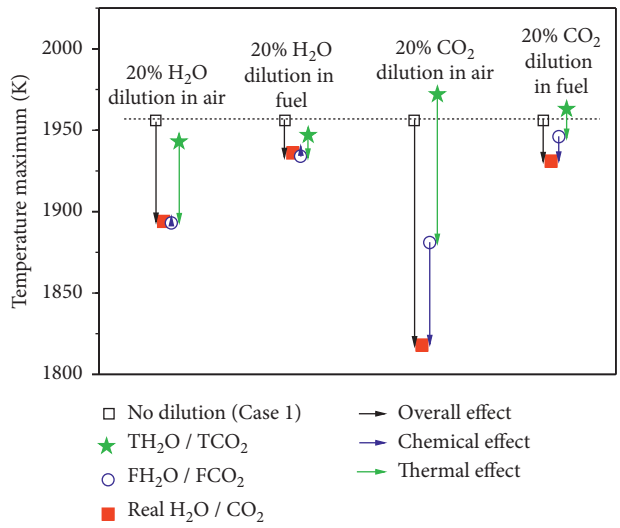

Figure 4: The overall and individual effects of 20% CO_2 and 20% H_2O dilution on the peak flame temperature of CH_4/air counterflow diffusion flame: $a_s = 50\ s^{-1}$, $L = 2$ cm, 400 K.

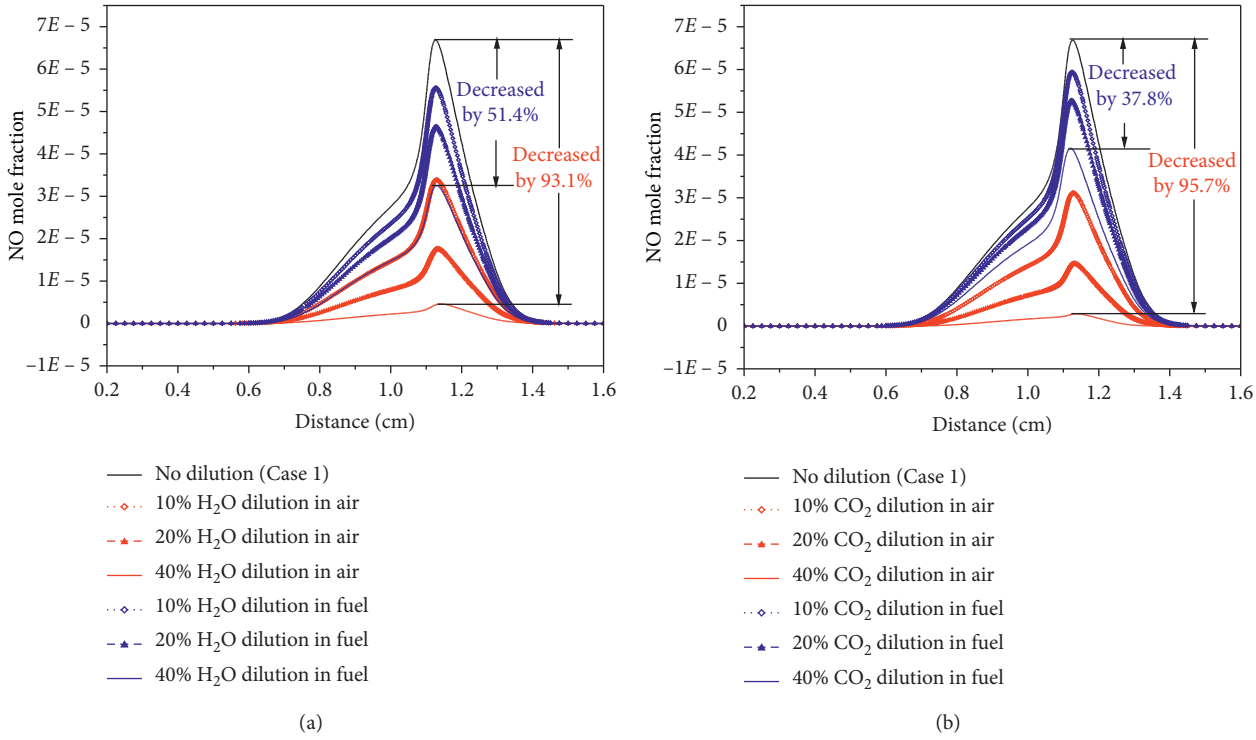

Figure 5: Distributions of NO mole fraction in CH_4/air counterflow diffusion flames as a function of distance from the fuel nozzle with H_2O, (a) and CO_2, (b) dilution: $a_s = 50\ s^{-1}$, $L = 2$ cm, 400 K.

since the prompt NO is the dominant NO formation route. This point will be discussed in more detail in Section 3.4.

Most simulations in this study were conducted at $T = 400$ K and $a_s = 50\ s^{-1}$. To show that the effects of dilution on NO reduction under these conditions are generalizable, Figures 7 and 8 exhibit the peak NO mole fraction at different strain rates (from 20 to 100 s^{-1}) and inlet temperature (from 400 to 600 K), and very similar trends can be found among the displayed lines. However, the detailed analyses of how strain rates and inlet temperature affects the NO formation are beyond this paper's scope.

Figure 9 displays the individual effects of 20% H_2O and 20% CO_2 dilution on the peak NO mole fraction. The dilution effects on NO reduction in the air-side are stronger than those in the fuel-side, same as the influence on flame temperature, Figure 4. In Figure 9, the chemical effect of H_2O dilution exerts a decreasing impact on NO emission despite promoting the flame temperature in Figure 4. This

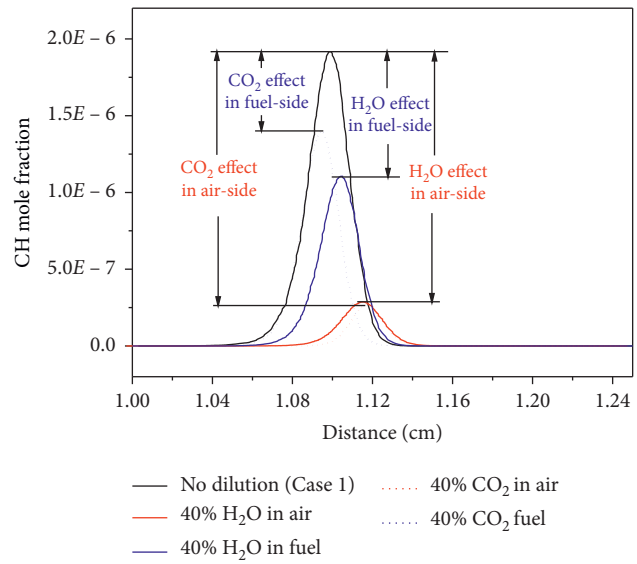

FIGURE 6: Distributions of CH mole fraction in CH_4/air counterflow diffusion flames with and without 40% H_2O and 40% CO_2 dilution on the air and fuel sides: $a_s = 50\ s^{-1}$, $L = 2$ cm, 400 K.

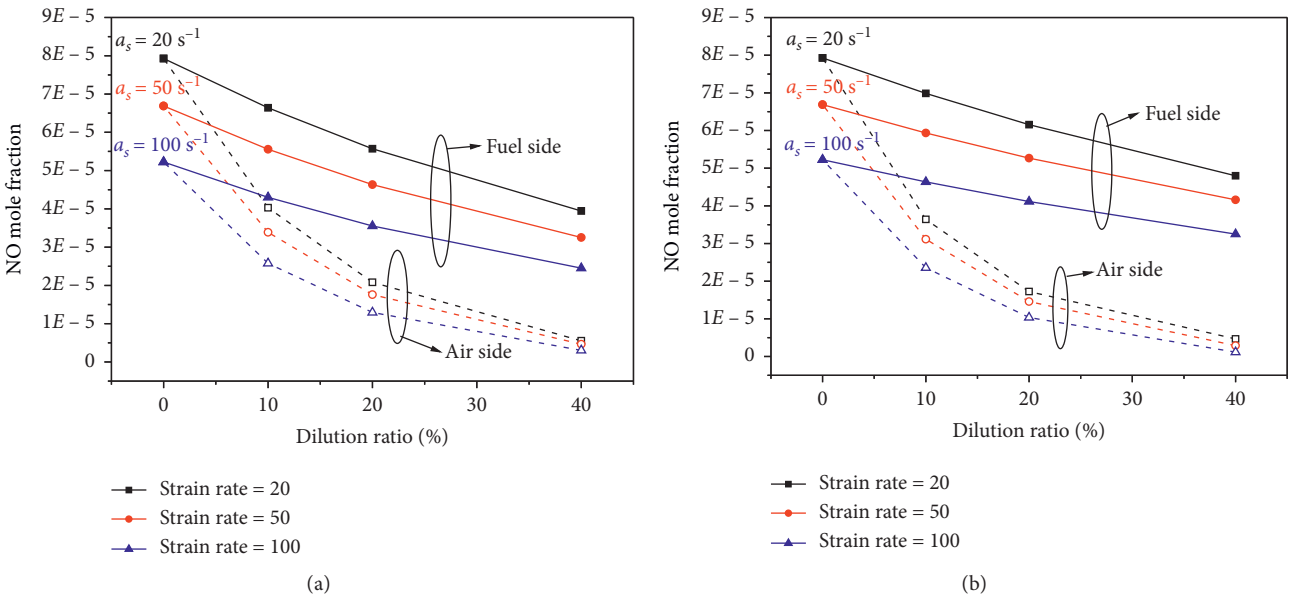

FIGURE 7: The peak NO mole fraction of CH_4/air counterflow diffusion flames with different strain rates: $a_s = 20\ s^{-1}$ (black), $50\ s^{-1}$ (red) and $100\ s^{-1}$ (blue). $L = 2$ cm, 400 K. (a) H_2O dilution. (b) CO_2 dilution.

can be easily understood from the distribution of CH radical shown in Figure 6. Although the flame temperature is enhanced slightly by H_2O dilution, the CH concentration is reduced more considerably, which results in more significant NO reduction through the prompt NO route than the prompting effect on NO through the thermal NO route.

3.4. NO Formation Mechanism. Figure 10 displays the emission index of NO via different formation routes as introduced in Section 2.3. The emission index of NO was calculated using equation (3), which has been widely utilized in previous studies, such as [10, 30].

$$\mathrm{EINO} = \frac{\int_0^L \omega_{\mathrm{NO}} M_{\mathrm{NO}} \mathrm{d}x}{-\int_0^L \omega_F M_F \mathrm{d}x}, \tag{3}$$

where ω_{NO} and ω_F are the NO production rate and fuel consumption rate, respectively, and M_{NO} and M_F are the molecular weight of nitric oxide and fuel, respectively.

Firstly, it can be observed that the effects of H_2O and CO_2 dilution in the air- or fuel-side on EINO correlate well

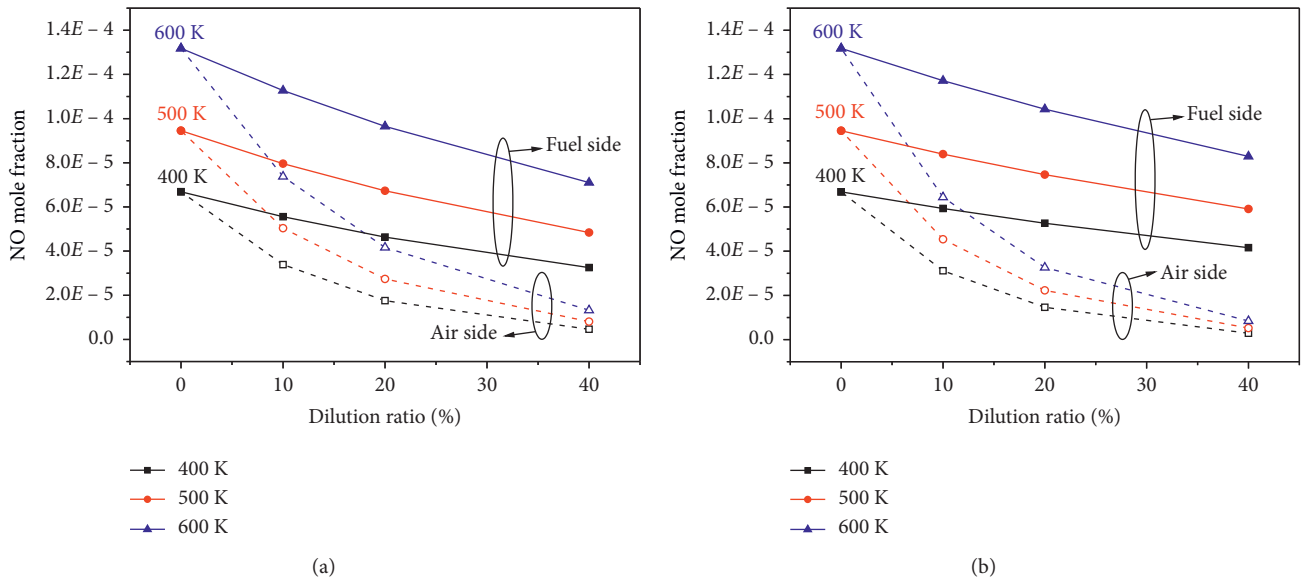

Figure 8: The peak NO mole fraction of CH_4/air counterflow diffusion flames with different inlet temperatures: $T = 400$ K (black), 500 K (red), and 600 K (blue). $a_s = 50\ s^{-1}$, $L = 2$ cm.

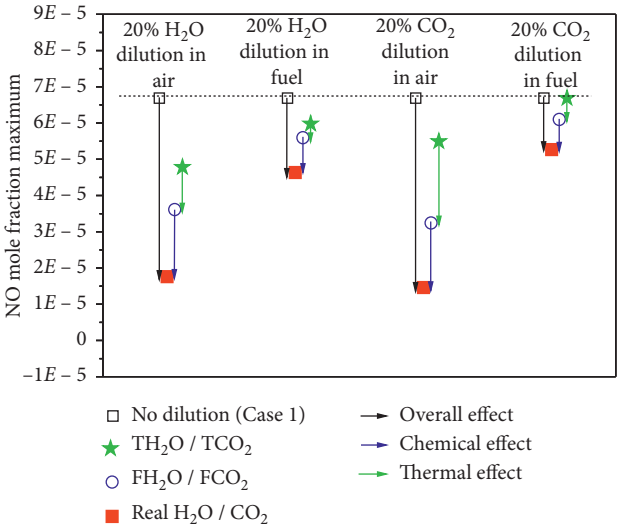

Figure 9: Peak NO mole fractions of CH_4/air counterflow diffusion flame with and without 20% H_2O and 20% CO_2 dilution: $a_s = 50\ s^{-1}$, $L = 2$ cm 400 K.

with those on the peak NO mole fraction shown in Figures 5 and 9, namely, air-side CO_2 dilution > air-side H_2O dilution > fuel-side H_2O dilution > fuel-side CO_2 dilution. This is because that CH_4 flow rate was kept constant for all the cases, and EINO was calculated over the entire computational domain in this study. Secondly, the prompt route plays the dominant role in NO formation, followed by the NO-reburning and NNH route, while the thermal and N_2O-intermediate routes contribute negligibly. For clarity, the percentages of reduction of total NO, prompt NO, NNH NO, and NO-reburning for 20% H_2O and 20% CO_2 dilution are also marked in Figure 10. For example, 18.8% means adding 20% CO_2 into the fuel stream (Case 6) reduces 18.8% NO emission than the no-dilution case (Case 1). It can be observed that the order of NO reduction percentage through the prompt NO route and NO-reburning for different dilutions totally agrees well with that through the full chemistry, i.e., air-side CO_2 dilution > air-side H_2O dilution > fuel-side H_2O dilution > fuel-side CO_2 dilution. However, H_2O and CO_2 dilution's influence on the third most important NO formation route (NNH pathway) does not follow the above order. Even so, it can still be concluded that the relative importance of H_2O and CO_2 dilution to NO formation reduction is determined by the dilution impact on the prompt NO formation and NO-reburning routes under the conditions of this study.

Using the method proposed by Revel et al. [32], the elemental fluxes of N through some critical reactions were calculated, and the pathways of NO formation based on the full chemistry of the GRI-Mech 2.11 for Case 1, Case 3, Case 6, Case 9, and Case 12 are demonstrated in Figure 11. It is worth pointing out that N's elemental fluxes were calculated along with the whole computational domain rather than just at the flame front, indicating the average value over the entire combustion process. In Figure 11, the arrow shows the progress direction of a certain conversion, from the reactants to the products. The values on each arrow indicate the N flux over the entirely computational domain (from the fuel nozzle exit to the oxidizer nozzle exit with a distance of 2 cm in this study), and the width of each arrow distinguishes the magnitude of the N flux. The percentage after the value means the ratio of the N flux reduction relative to the baseline case (Case 1) through the reaction after it in parentheses. The pathway map in Figure 11 covers the five NO formation/destruction routes, and the conversion paths can be briefly highlighted as the thermal route ($N_2 \longrightarrow N \longrightarrow NO$), prompt route ($N_2 \longrightarrow HCN \longrightarrow CN$, NCO, NH, N, and $HNO \longrightarrow NO$), NNH route ($N_2 \longrightarrow NNH$

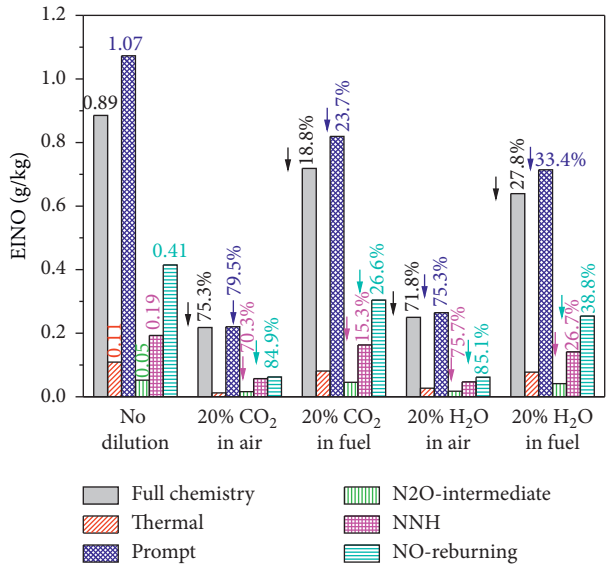

FIGURE 10: The percentages of EINO reduction by 20% H_2O and 20% CO_2 dilution in the air and fuel side of CH_4/air counterflow diffusion flame: $a_s = 50\ s^{-1}$, $L = 2$ cm, 400 K.

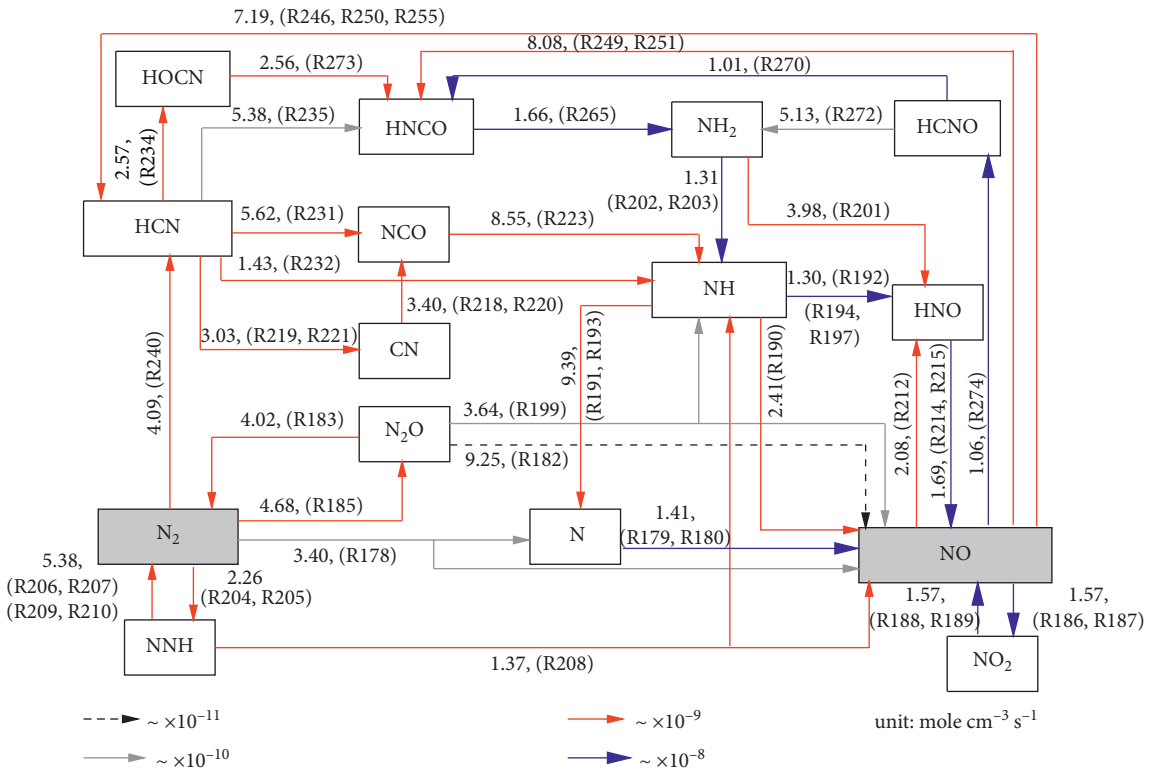

(a)

FIGURE 11: Continued.

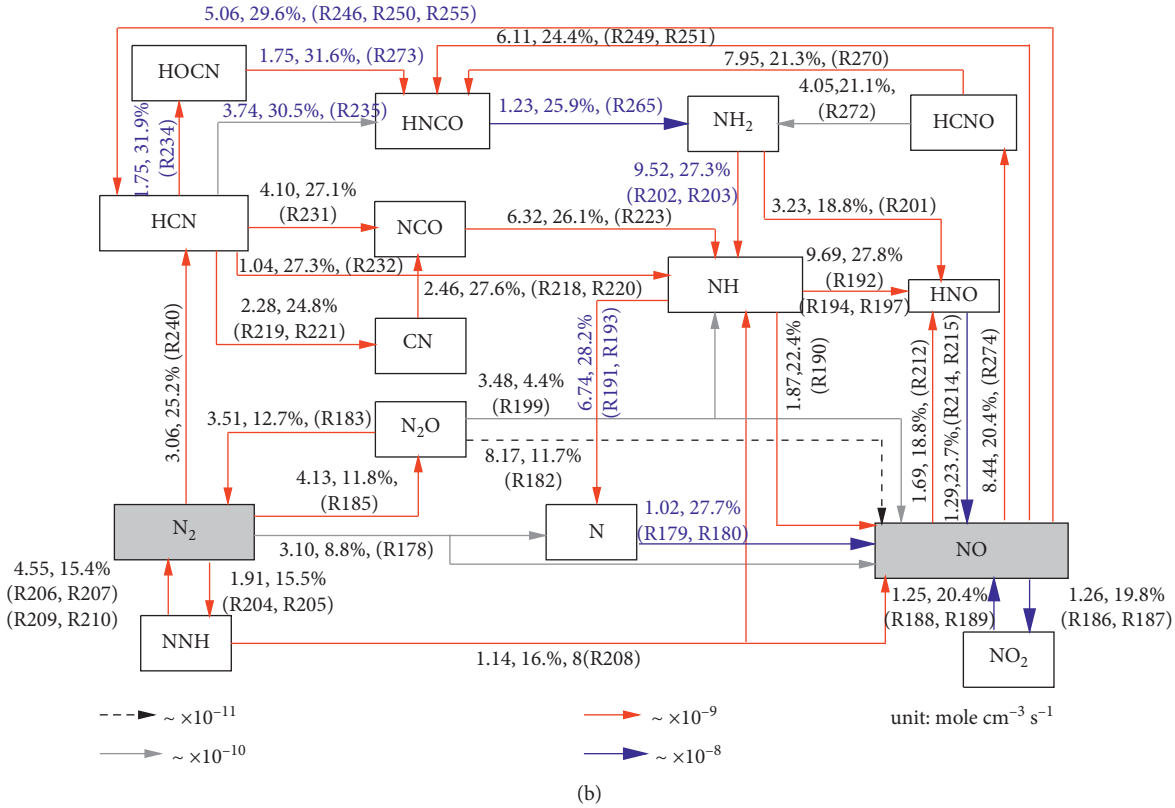

(b)

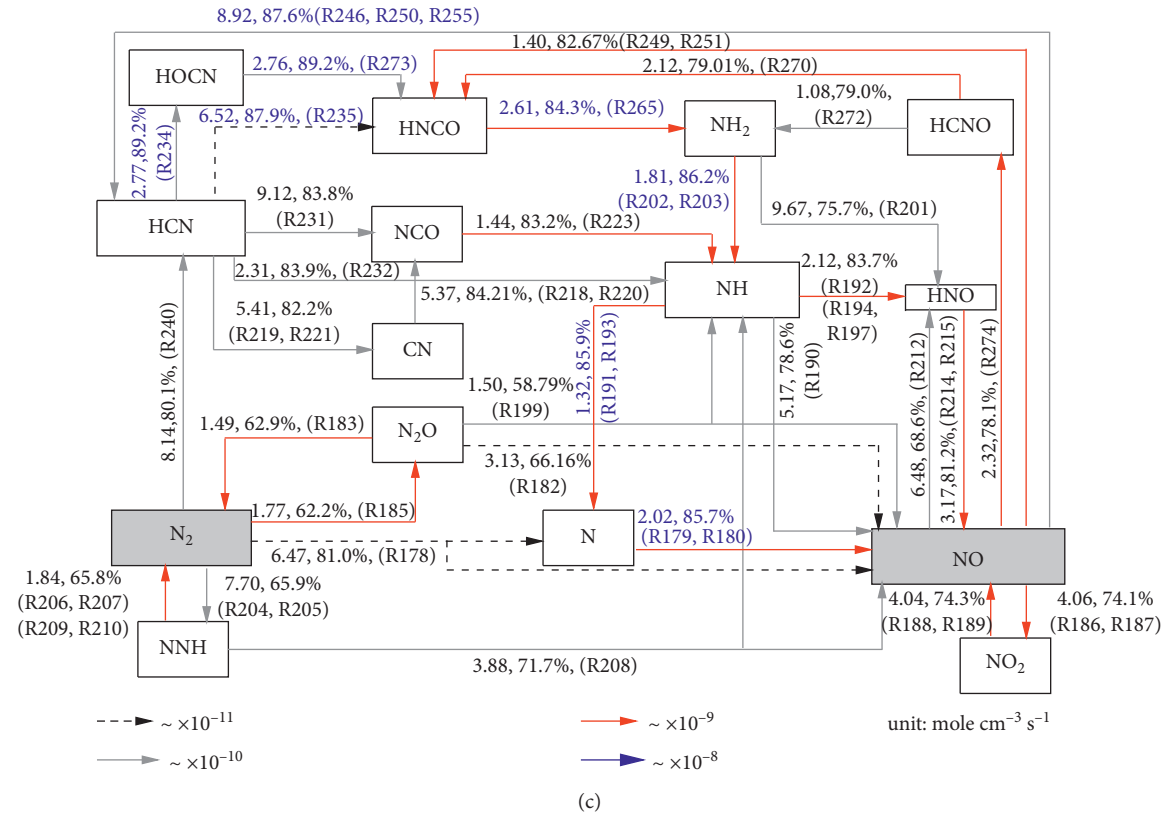

(c)

Figure 11: Continued.

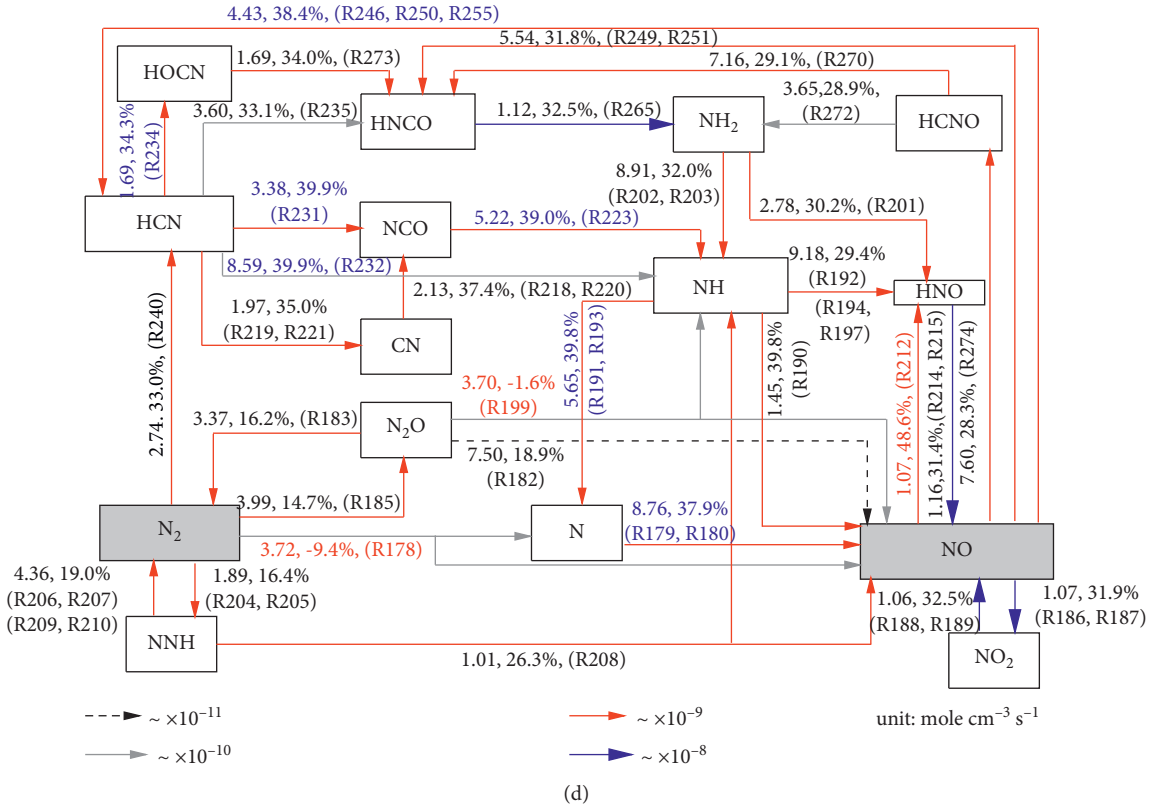

(d)

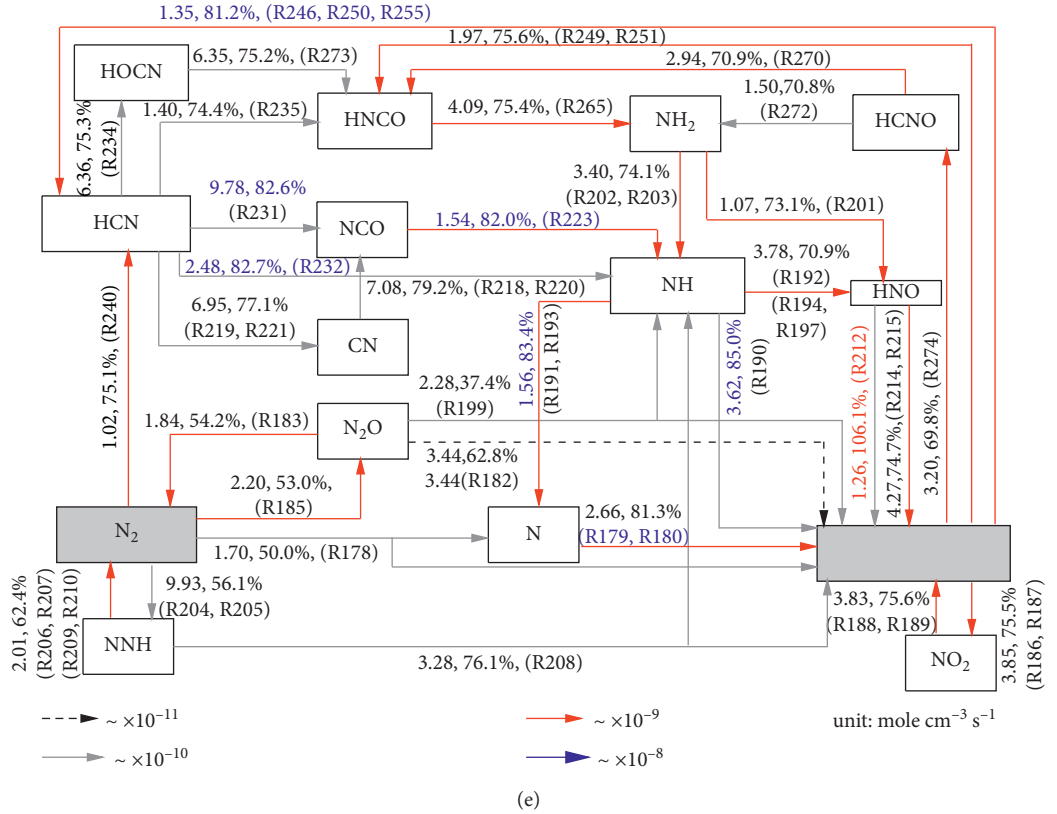

(e)

Figure 11: NO formation pathways for (a) no dilution (Case 1). (b) 20% CO_2 dilution in fuel (Case 6). (c) 20% CO_2 dilution in air (Case 12). (d) 20% H_2O dilution in fuel (Case 3). (e) 20% H_2O dilution in air (Case 9).

(⟶NH)⟶NO), N_2O-intermediate route (N_2⟶N_2O (⟶NH) ⟶NO), and part of NO-reburning route (N_2⟶HCN, HCNO⟶CN, NCO, NH_3, NH_2, NH,⟶N_2O, NO, and N_2).

By comparing Figures 11(b) and 11(c) with Figures 11(a), 11(d) and 11(e) with Figure 11(a), it can be found that the air-side dilution and fuel-side dilution affect the NO formation pathway similarly in general. To be specific, the nitrogen elemental fluxes in Figure 11(a) are the highest among all the five presented cases, indicating that the CH_4 flame without dilution produces the highest amount of NO. The fuel-side dilution weakens the nitrogen elemental fluxes to a lesser degree than the air-side dilution for both H_2O and CO_2 diluents. Besides, as a more detailed illustration than Figure 10, Figure 11 shows that the NO formation through the thermal route, NNH route, and N_2O-intermediate route is much less influenced than that through the prompt route, and the less affected reactions include R204 to R210 (NNH route), R178 (thermal route), and R185, R183, R182, and R199 (N_2O-intermediate route).

However, differences do exist between the effects of the two diluents. When the flame is diluted with CO_2, the NO formation pathway, NO⟶HCN (⟶HOCN)⟶HNCO⟶NH_2⟶NH⟶N⟶NO (the N flux and its reduction percentage, as well as the involved reactions, are distinguished in blue), is most affected. While for H_2O dilution, the most affected pathway is NO⟶HCN (⟶NCO)⟶NH (⟶N)⟶NO. Besides, another remarkable change for H_2O dilution can be observed for the conversion of NO⟶HNO. When H_2O is added to the fuel-side, the nitrogen elemental flux of R212 (from the NNH NO formation route) is decreased mainly by 48.56%. This degree far exceeds that of other NO formation pathways (with reduction percentages of 14.74%–39.93%). As for H_2O dilution on the air-side, the direction of the conversion between NO and HNO is even reversed. This shift of the progress direction of R212 correlates well with the highest NO reduction percentage of air-side H_2O dilution in Figure 8. All the abovementioned phenomena show that H_2O dilution has more complex influences on flame structure and NO formation reduction than CO_2 dilution.

4. Conclusions

Motivated by the widespread utilization of dilution combustion in many advanced technologies, this work systematically compared the effects of up to 40% H_2O and CO_2 dilutions to the fuel- and air-side on NO emissions in N_2 diluted CH_4/air counterflow diffusion flames. This numerical study was performed using the OPPDIF code in conjunction with the GRI-Mech 2.11 kinetics mechanism at varying strain rates (20–100 s^{-1}) and inlet temperatures range from 400 K to 800 K, 1 atm. The dilution was also realized by replacing N_2 with either CO_2 or H_2O in the oxidizer and the fuel stream to maintain the fuel and oxygen concentration constant. Several important findings are listed as follows:

(1) The dilutions with H_2O and CO_2 in the oxidizer and fuel-side all decrease the flame temperature and NO formation. Dilutions by H_2O and CO_2 lower the peak flame temperature nearly linearly as the dilution ratio increases. The reduction rate of peak NO mole fraction displays a decreasing trend with increasing the dilution ratio, especially when the dilution takes place on the oxidizer side. The differences between the results based on the adiabatic treatment, the optically thin approximation, and the discrete-ordinates method coupled with the statistical narrow-band based correlated-k radiative property model decrease with increasing the dilution ratio.

(2) The chemical effects of CO_2 dilution lower both the flame temperature and NO emissions while the chemical effect of H_2O dilution exerts a slightly promoting impact on the flame temperature but a suppression influence on NO formation. The apparently conflicting chemical effect of H_2O dilution on the flame temperature and NO formation is attributed to the considerably suppressed CH radical, which results in more significant NO reduction through the dominant prompt NO route than the NO promotion through the thermal NO route.

(3) The importance of effects of H_2O and CO_2 dilution in the air- and fuel-side on NO reduction follows the order of air-side CO_2 dilution > air-side H_2O dilution > fuel-side H_2O dilution > fuel-side CO_2 dilution, and the prompt NO route always plays the dominant role under the current investigation conditions.

(4) Pathway analysis shows that the air-side dilution and fuel-side dilution affect the NO formation pathway similarly in general, but H_2O dilution still differs from CO_2 dilution. When the flame is diluted with CO_2, the most affected NO formation pathway is NO⟶HCN (⟶HOCN)⟶HNCO⟶NH_2⟶NH⟶N⟶NO. However, when the flame is diluted with H_2O, the most affected pathway is NO⟶HCN (⟶NCO)⟶NH (⟶N)⟶NO.

Data Availability

The data used to support the findings of this study are available from the corresponding author upon request.

Conflicts of Interest

The authors declare that they have no conflicts of interest.

Acknowledgments

This work was supported by the National Natural Science Foundation of China (51776112), China Postdoctoral Science Foundation (2020M672059), the Fundamental Research Funds of Shandong University, Shandong Provincial Natural Science Foundation of China (Grant no. ZR2020QE198), and the Fundamental Research Funds for the Central Universities

(18CX02129A). The authors sincerely acknowledge these financial supports.

References

[1] M. Jonsson and J. Yan, "Humidified gas turbines-a review of proposed and implemented cycles," *Energy*, vol. 30, no. 7, pp. 1013–1078, 2005.

[2] H. Jericha, W. Sanz, and E. Gottlich, "Design concept for large output graz cycle gas turbines," *Turbo Expo: Power for Land, Sea, and Air*, pp. 1–14, American Society of Mechanical Engineers, New York, NY, USA, 2006.

[3] G. H. Abd-Alla, "Using exhaust gas recirculation in internal combustion engines: a review," *Energy Conversion and Management*, vol. 43, no. 8, pp. 1027–1042, 2002.

[4] R. W. Bilger and Z. Wu, "Carbon capture for automobiles using internal combustion Rankine cycle engines," *Journal of Engineering for Gas Turbines and Power*, vol. 131, no. 3, pp. 034502–034505, 2009.

[5] S. Hoseinzadeh, S. Ghasemi, and S. Heyns, "Application of hybrid systems in solution of low power generation at hot seasons for micro hydro systems," *Renewable Energy*, vol. 160, pp. 323–332, 2020.

[6] S. Hoseinzadeh and S. Heyns, "Advanced energy, exergy and environmental (3E) analyses and optimization of a coal-fired 400 MW thermal power plant," *Journal of Energy Resources Technology*, vol. 143, no. 8, p. 082106, 2021.

[7] L. Wang, Z. Liu, S. Chen, C. Zheng, and J. Li, "Physical and chemical effects of CO_2 and H_2O additives on counterflow diffusion flame burning methane," *Energy & Fuels*, vol. 27, no. 12, pp. 7602–7611, 2013.

[8] H. Xu, F. Liu, S. Sun, Y. Zhao, S. Meng, and W. Tang, "Effects of H_2O and CO_2 diluted oxidizer on the structure and shape of laminar coflow syngas diffusion flames," *Combustion and Flame*, vol. 177, pp. 67–78, 2017.

[9] L. Zhuo, Y. Jiang, R. Qiu, J. An, and W. Xu, "Effects of fuel-side N2, CO2, H2O dilution on combustion characteristics and NOx formation of syngas turbulent nonpremixed jet flames," *Journal of Engineering for Gas Turbines and Power*, vol. 136, no. 6, pp. 061505–061511, 2014.

[10] J. Park, S.-G. Kim, K.-M. Lee, and T. K. Kim, "Chemical effect of diluents on flame structure and NO emission characteristic in methane-air counterflow diffusion flame," *International Journal of Energy Research*, vol. 26, no. 13, pp. 1141–1160, 2002.

[11] Y. Xie, J. Wang, N. Xu, S. Yu, and Z. Huang, "Comparative study on the effect of CO2 and H2O dilution on laminar burning characteristics of CO/H2/air mixtures," *International Journal of Hydrogen Energy*, vol. 39, no. 7, pp. 3450–3458, 2014.

[12] D. Ning, A. Fan, and H. Yao, "Effect of radiation emission and reabsorption on flame temperature and NO formation in H2/CO/air counterflow diffusion flames," *International Journal of Hydrogen Energy*, vol. 42, no. 34, pp. 22015–22026, 2017.

[13] S. Öztürk, "The effects of CO2, N2, and H2O dilutions on NO formation of partially premixed synthesis gas combustion," *Cumhuriyet Science Journal*, vol. 40, no. 4, pp. 813–818, 2019.

[14] J. J. Feese and S. R. Turns, "Nitric oxide emissions from laminar diffusion flames: effects of air-side versus fuel-side diluent addition," *Combustion and Flame*, vol. 113, no. 1-2, pp. 66–78, 1998.

[15] E.-S. Cho and S. H. Chung, "Characteristics of NOx emission with flue gas dilution in air and fuel sides," *KSME International Journal*, vol. 18, no. 12, pp. 2303–2309, 2004.

[16] B. Rahmanian, M. R. Safaei, S. N. Kazi, G. Ahmadi, H. F. Oztop, and K. Vafai, "Investigation of pollutant reduction by simulation of turbulent non-premixed pulverized coal combustion," *Applied Thermal Engineering*, vol. 73, no. 1, pp. 1222–1235, 2014.

[17] Z. Abdelmalek, R. Alamian, M. S. Shadloo, A. Maleki, and A. Karimipour, "Numerical study on the performance of a homogeneous charge compression ignition engine fueled with different blends of biodiesel," *Journal of Thermal Analysis and Calorimetry*, pp. 1–11, 2020.

[18] R. S. Gavhane, A. M. Kate, A. Pawar et al., "Effect of zinc oxide nano-additives and soybean biodiesel at varying loads and compression ratios on VCR diesel engine characteristics," *Symmetry*, vol. 12, no. 6, p. 1042, 2020.

[19] M. K. Chernovsky, A. Atreya, and H. G. Im, "Effect of CO_2 diluent on fuel versus oxidizer side of spherical diffusion flames in microgravity," *Proceedings of the Combustion Institute*, vol. 31, no. 1, pp. 1005–1013, 2007.

[20] J. Park, D.-J. Hwang, J.-G. Choi, K.-M. Lee, S.-I. Keel, and S.-H. Shim, "Chemical effects of CO2 addition to oxidizer and fuel streams on flame structure in H_2-O_2 counterflow diffusion flames," *International Journal of Energy Research*, vol. 27, no. 13, pp. 1205–1220, 2003.

[21] F. Liu, H. Guo, G. J. Smallwood, and Ö. L. Gülder, "The chemical effects of carbon dioxide as an additive in an ethylene diffusion flame: implications for soot and NOx formation," *Combustion and Flame*, vol. 125, no. 1-2, pp. 778–787, 2001.

[22] A. E. Lutz, R. J. Kee, J. F. Grcar, and F. M. Rupley, *OPPDIF: a fortran program for computing opposed-flow diffusion flames*, Sandia National Laboratories, Livermore, CA, USA, 1997.

[23] R. J. Kee, F. M. Rupley, and J. A. Miller, *Chemkin-II: A Fortran Chemical Kinetics Package for the Analysis of Gas-phase Chemical Kinetics*, Sandia National Laboratories, Livermore, CA, USA, 1989.

[24] C. Bowman, R. Hanson, D. Davidson et al., "GRI-mech 2.11, 1995," 1995, http://www.me.berkeley.edu/gri_mech.

[25] S. H. Kim, K. Y. Huh, and B. Dally, "Conditional moment closure modeling of turbulent nonpremixed combustion in diluted hot coflow," *Proceedings of the Combustion Institute*, vol. 30, no. 1, pp. 751–757, 2005.

[26] K. W. Lee and D. H. Choi, "Prediction of NO in turbulent diffusion flames using Eulerian particle flamelet model," *Combustion Theory and Modelling*, vol. 12, no. 5, pp. 905–927, 2008.

[27] S. R. Turns, *Introduction to Combustion*, McGraw-Hill Companies, New York, NY, USA, 1996.

[28] F. Liu, H. Guo, G. Smallwood, and M. El Hafi, "Effects of gas and soot radiation on soot formation in counterflow ethylene diffusion flames," *Journal of Quantitative Spectroscopy and Radiative Transfer*, vol. 84, no. 4, pp. 501–511, 2004.

[29] D. E. Giles, S. Som, and S. K. Aggarwal, "NOx emission characteristics of counterflow syngas diffusion flames with airstream dilution," *Fuel*, vol. 85, no. 12-13, pp. 1729–1742, 2006.

[30] F. Wang, P. Li, J. Zhang, Z. Mei, J. Mi, and J. Wang, "Routes of formation and destruction of nitrogen oxides in CH4/H2 jet flames in a hot coflow," *International Journal of Hydrogen Energy*, vol. 40, no. 18, pp. 6228–6242, 2015.

[31] S. J. Klippenstein, L. B. Harding, P. Glarborg, and J. A. Miller, "The role of NNH in NO formation and control," *Combustion and Flame*, vol. 158, no. 4, pp. 774–789, 2011.

[32] J. Revel, J. Boettner, M. Cathonnet, and J. Bachman, "Derivation of a global chemical kinetic mechanism for methane ignition and combustion," *Journal de chimie physique*, vol. 91, pp. 365–382, 1994.